NEURAL REGENERATION RESEARCH
October 2015, Volume 10, Issue 10
www.nrronline.org

RESEARCH ARTICLE

Electrospun and woven silk fibroin/poly(lactic-co-glycolic acid) nerve guidance conduits for repairing peripheral nerve injury

Ya-ling Wang[1, 2], Xiao-mei Gu[3], Yan Kong[4], Qi-lin Feng[5], Yu-min Yang[1, 4, *]

1 Key Laboratory of Eco-Textiles, Ministry of Education, Jiangnan University, Wuxi, Jiangsu Province, China
2 School of Chemistry and Chemical Engineering, Nantong University, Nantong, Jiangsu Province, China
3 Jiangsu College of Engineering and Technology, Nantong, Jiangsu Province, China
4 Jiangsu Key Laboratory of Neuroregeneration, Nantong University, Nantong, Jiangsu Province, China
5 School of Medicine, Nantong University, Nantong, Jiangsu Province, China

***Correspondence to:**
Yu-min Yang, M.D., yangym@ntu.edu.cn.

orcid:
0000-0002-7390-5842 (Yu-min Yang)

doi: *10.4103/1673-5374.167763*
http:*//www.nrronline.org/*

Accepted: *2015-06-10*

Abstract

We have designed a novel nerve guidance conduit (NGC) made from silk fibroin and poly(lactic-co-glycolic acid) through electrospinning and weaving (ESP-NGCs). Several physical and biological properties of the ESP-NGCs were assessed in order to evaluate their biocompatibility. The physical properties, including thickness, tensile stiffness, infrared spectroscopy, porosity, and water absorption were determined *in vitro*. To assess the biological properties, Schwann cells were cultured in ESP-NGC extracts and were assessed by morphological observation, the MTT assay, and immunohistochemistry. In addition, ESP-NGCs were subcutaneously implanted in the backs of rabbits to evaluate their biocompatibility *in vivo*. The results showed that ESP-NGCs have high porosity, strong hydrophilicity, and strong tensile stiffness. Schwann cells cultured in the ESP-NGC extract fluids showed no significant differences compared to control cells in their morphology or viability. Histological evaluation of the ESP-NGCs implanted *in vivo* indicated a mild inflammatory reaction and high biocompatibility. Together, these data suggest that these novel ESP-NGCs are biocompatible, and may thus provide a reliable scaffold for peripheral nerve repair in clinical application.

Key Words: *nerve regeneration; peripheral nerve injury; poly(lactic-co-glycolic acid); electrospinning; silk fibroin; biocompatibility; nerve guidance conduit; weaving*

Funding: *This study was supported by the National Natural Science Foundation of China, No. 81371687, 81171457.*

Wang YL, Gu XM, Kong Y, Feng QL, Yang YM (2015) Electrospun and woven silk fibroin/poly(lactic-co-glycolic acid) nerve guidance conduits for repairing peripheral nerve injury. Neural Regen Res 10(10):1635-1642.

Introduction

Peripheral nerve repair is one of the most difficult problems in the field of neuroscience. When a nerve defect gap is too wide to suture end-to-end, implantation of a nerve graft is often necessary in order to bridge the proximal and distal nerve stumps and to promote nerve regeneration. A nerve autograft harvested from a different site in the body is often used to repair large nerve gaps. However, this technique has many limitations, such as tissue availability, donor site morbidity, and secondary deformities, as well as the potential differences in tissue structure and size (Ducker and Hayes, 1970; Evans, 2000). Artificial nerve guidance conduits (NGCs) are good alternatives to traditional nerve autografts. An ideal NGC is biocompatible and shows appropriate biodegradability, as well as the desired mechanical properties and a sufficient permeability.

In recent years, many synthetic and natural biopolymers including polyglycolic acid, polylactic acid, chitosan, alginate and their composites and derivatives have been used to fabricate NGCs (Suzuki et al., 2000; Weber et al., 2000; Fabre et al., 2001; Yuan et al., 2004; Wang et al., 2005). Poly(lactic-co-glycolic acid) (PLGA) has been extensively used as a carrier for drug delivery and as a scaffold for tissue engineering applications (Kim et al., 2007; Lee et al., 2009; Jin et al., 2010; Felix Lanao et al., 2011; Guo et al., 2011).

Silk fibroin (SF) has appropriate mechanical, structural, biodegradable, and biocompatible properties (Santin et al., 1999; Shao and Vollrath, 2002; Altman et al., 2003). It is a promising biomaterial with applications in a broad variety of biomedical fields, especially for tissue engineering of artificial bones, tendon, cartilage, and peripheral nerve regeneration (Gotoh et al., 2004; Unger et al., 2004; Yamada et al., 2004; Bayraktar et al., 2005; Dal Pra et al., 2005; Uebersax et al., 2006; Yang et al., 2007b).

We previously reported that SF fibers and SF conduits with nerve tissues and cells are biocompatible and biodegradable

in vitro and *in vivo* (Chen et al., 2007; Tang et al., 2009; Yang et al., 2009). We also determined the mechanical properties and permeability of NGCs that were made from SF through lyophilization, referred to as SF-NGCs, and further investigated the feasibility of using SF-NGCs to bridge 10 mm sciatic neural defects in rats (Yang et al., 2007b).

The fabrication of three-dimensional scaffolds that mimic the cellular microenvironment is an important goal for the success of tissue-engineered constructs (Vozzi et al., 2003). Electrospinning techniques have attracted a significant amount of attention during the last several years because they are simple and straightforward methods to produce fibrous and microporous scaffolds (Choi et al., 2008).

Here, we report the design of novel NGCs made from SF and PLGA (ESP-NGCs) through electrospinning and weaving. We hypothesized that the designed conduit with electrospun nanoporous structure and an embedded reinforcing weaving net would possess desirable biological and mechanical properties. To test this hypothesis, we cultured Schwann cells in ESP-NGC extracts in order to evaluate their *in vitro* cytotoxicity, and subcutaneously implanted ESP-NGCs in rabbits to examine their *in vivo* biocompatibility.

Materials and Methods

Preparation of ESP-NGCs

Bombyx mori silk, purchased from sericulture provider Xinyuan Co., Ltd. (Hai'an, Jiangsu, China), was boiled three times in 0.5% $NaCO_3$ solution for 0.5 hours each time. After washing with distilled water several times, the degummed silk fibers were first dissolved in a ternary solvent system of $CaCl_2/H_2O/C_2H_5OH$ (molar ration 1:8:2) at 75 ± 2°C in a thermostatic bath, and then dialyzed against distilled water in a cellulose tube (molecular cutoff: 12,000–14,000 Da) at room temperature for 3 days (Chen et al., 2006; Yang et al., 2009). A portion of the obtained SF aqueous solution was cast in a stainless steel tray, and then the tray was dried at room temperature to form the SF membrane.

The ESP-NGCs were fabricated using a custom-designed electrospinning apparatus. The SF membranes were dissolved in formic acid to a concentration of 13–15%. The solution was placed in a 2.0 mL glass syringe with a blunt-ended needle (inner diameter: 0.9 mm). A voltage of 22–25 kV was applied to the needle and the flow rate was 2 mL/h. The SF fibers were collected on a rotating stainless steel rod (diameter: 2 mm; rotation speed: 500 r/min), which was approximately 10–15 cm away from the tip of the needle.

Once the desired thickness of SF nanofibers was deposited on the mandrel rod (**Figure 1A**), the PLGA suture was weaved onto the SF (**Figure 1B**). The electrospinning was then continued until another layer of SF nanofibers with the desired thickness was deposited (**Figure 1C**). After being treated with ethanol for 20 minutes, the fabricated ESP-NGCs were dried under a vacuum at room temperature.

Characterization of the ESP-NGCs

Scanning electron microscopy

A Philips XL-30 scanning electron microscope (SEM; Eindhoven, the Netherlands) was used to observe the morphology of the electrospun nanofibers and ESP-NGCs. Before testing, the samples were coated with gold using a JEOL JFC-110E Ion Sputter system.

Fourier transform infrared spectroscopy

After the samples were cleaned with ethanol and dried, the sample powder was pelleted with potassium bromide (KBr) and analyzed using a model Nexus 870 Fourier transform infrared (FTIR) spectrophotometer (Nicolet Instruments Co., Madison, WI, USA). All spectra were taken in the spectral range of 4,000–500 cm^{-1}.

Porosity

The liquid displacement method was used to measure the porosity of the ESP-NGCs. Hexane was used as a displacement liquid because it permeates through the ESP-NGCs without swelling or shrinking the matrix (Kim et al., 2005). ESP-NGCs with a defined mass were immersed in a known volume (V_1) of hexane in a graduated cylinder for 5 minutes. The total volume of the hexane plus that of the hexane-impregnated ESP-NGC was recorded as V_2. The hexane-impregnated ESP-NGC was then removed from the cylinder, and the residual hexane volume was recorded as V_3. The total volume of the ESP-NGC was calculated as: $V = (V_2 - V_1) + (V_1 - V_3) = V_2 - V_3$, where $(V_2 - V_1)$ is the volume of the ESP-NGC and $(V_1 - V_3)$ is the volume of hexane within the ESP-NGC. The porosity of the ESP-NGC (ε) was calculated as: $\varepsilon\ (\%) = (V_1 - V_3) / (V_2 - V_3) \times 100$.

Swelling property

The ESP-NGCs were immersed in phosphate buffered saline (PBS; pH 7.4) at room temperature for 24 hours. The swelling ratio of the ESP-NGC was calculated as: Swelling ratio $(\%) = (m_2 - m_1)/ m_1 \times 100$, where m_1 is the dry sample mass and m_2 is the wet sample mass.

Mechanical testing

The tensile strength and transverse compression strength of the ESP-NGCs were measured on a J-100N strength-testing machine (Languang Mechanics and Electronics Technology Development Center, Jinan, China) while with samples were kept hydrated in PBS (pH 7.4) at 37°C. The sample length was 10 mm. The tensile test speed was 10 mm/min and the gauge length was 60 mm. The crosshead speed was maintained at 1.0 mm/min.

Biocompatibility *in vitro*

Preparation of extract fluids

The ESP-NGCs were placed in an extraction container with Dulbecco's modified Eagle's medium (DMEM; Sigma Aldrich, St. Louis, MO, USA) and incubated at 37°C for 72 ± 0.5 hours (Fini et al., 2005). The resulting extract fluid was used within 24 hours. As controls, extraction fluids from hydroxyapatite (Sigma) and organotin (Hongding Chemicals Company, Nantong, Jiangsu, China) were prepared in the same manner. All of the operations were performed under sterile conditions.

Isolation of rat Schwann cells

Rat Schwann cells (rSCs) were harvested for cell culture as follows. Primary rSCs were isolated from the sciatic nerves and dorsal root ganglia (DRG) of neonatal (1–2 days old) Sprague-Dawley rats obtained from the Laboratory Animal Center of Nantong University, Jiangsu Province, China. All animal protocols were approved by the Administration Committee of Experimental Animals, Jiangsu Province, China. The rSCs were then purified using a method modified from Brockes (Weinstein and Wu, 2001). First, the harvested nerve tissues were sheared into fragments and digested in 0.25% trypsin for 30 minutes. Dulbecco's modified Eagle medium (DMEM) supplemented with 10% fetal bovine serum (FBS) and 100 U/mL penicillin and 100 μg/mL streptomycin (complete medium) was then added to stop the digestion process, and the tissues were washed twice in complete medium. The cells obtained were seeded onto poly-L-lysine pre-coated dishes with complete medium and were then incubated at 37°C in a humidified, 5% CO_2 atmosphere. After 24 hours, the medium was replaced by fresh complete medium supplemented with 10 μM cytosine arabinoside (Sigma), and the incubation was continued for another 24 hours. Then, the rSCs were cultured in complete medium containing 2 μM forsklin (Sigma) and 2 ng/mL heregulin (Sigma). To increase cell purity, they were treated with anti-Thy1 antibody (1:1,000; AbD Serotec, Raleigh, NC, USA) and complement (Jackson Immuno, West Grove, PA, USA).

Culture of rat Schwann cells

The purified rSCs were seeded into 96-well plates at a cell density of 1×10^4 cells/well, and the wells were assigned to different groups and treated with ESP-NGC extract fluid, hydroxyapatite extract fluid, organotin extract fluid, or complete medium. At different times during culture, the morphology of the rSCs in these different culture media was observed under an inverted light microscope (IX-70, Olympus Co., Tokyo, Japan).

MTT assay

The viability of rSCs cultured in the extract fluids or complete medium were determined using the colorimetric 3-(4,5-dimethylthiazol-2-yl)-2,5-diphenyltetrazolium bromide (MTT) assay (Bio-Tek Inc., Burlington, VT, USA). Aqueous solutions of MTT are yellowish, and the MTT is reduced by the mitochondrial dehydrogenases present in living cells. The viability of the rSCs was assessed at 12, 24, 48, and 72 hours and 7 days after culture in the different media. The cell culture media was replaced with MTT solution to a final concentration of 0.5 mg/mL, and the cells were incubated at 37°C for 4 hours. Then, a solution of sodium dodecyl sulfate was added to dissolve the formazan precipitate for 20 hours, and the optical density was measured at 570 nm on an ElX-800 microelisa reader (Bio-Tek Inc.).

Immunocytochemistry

After 1 or 3 days of culturing the rSCs in the ESP-NGCs extracts or complete medium, the samples were fixed in 4% paraformaldehyde for 30 minutes at room temperature, washed three times with PBS, and then blocked in 10% goat serum, 3% bovine serum albumin, and 0.1% Triton-X 100 for 1 hour. Next, they were incubated with mouse anti-rat S-100 monoclonal antibody (1:400; Sigma) and rabbit anti-β-tubulin III antibody (1:400; Sigma) overnight at 4°C in a humidified chamber. After being washed three times with PBS, the samples were further reacted with a mixture of tetraethyl rhodamine isothiocyanate (TRITC)-labeled goat anti-mouse IgG (1:200; Sigma) and FITC-labeled goat anti-rabbit IgG (1:200; Sigma) for 24 hours at 4°C. After three washes with PBS, the samples were stained with 5 μg/mL Hoechst 33342 (Sigma) at 37°C for 30 minutes, and washed three more times with PBS. All of the samples were imaged on a fluorescence microscope (Leica, Wetzlar, Germany).

Biocompatibility *in vivo*

The *in vivo* biocompatibility of the ESP-NGCs was tested by subcutaneously implanting them into ten New Zealand adult rabbits (mixed sex, 2.5–3.0 kg each) obtained from the Laboratory Animal Center of Nantong University, Jiangsu Province, China. All animal protocols were approved by the Administration Committee of Experimental Animals, Jiangsu Province, China.

The ESP-NGCs were cut into 10 mm segments and sterilized before use. The rabbits were anesthetized with 3% pentobarbital by ear vein injection. Then, the ESP-NGCs were subcutaneously implanted into the back of the rabbits, with three samples placed on each side. The surgical incisions were sutured closed.

After 4, 8, 12, and 24 weeks, the rabbits were sacrificed to harvest the implants for analysis. The harvested ESP-NGCs were fixed in 4% paraformaldehyde for 24 hours at 4°C, dehydrated through a 10%, 20%, and 30% sucrose gradient, embedded in 5% sucrose, and cut into 10 μm-thick sections. Hematoxylin-eosin staining was performed to visualize any tissue reactions to the implants. The integrity of the conduits and the inflammatory responses were observed under the light microscope (Leica).

Statistical analysis

The data were analyzed using SPSS 11.5 (SPSS, Chicago, IL, USA). Differences between groups were assessed using one-way analysis of variance, and *P*-values less than 0.05 were considered statistically significant. The results are expressed as the mean ± standard deviation (SD).

Results

Physical characteristics

Characterization of the ESP-NGCs

Tubular ESP-NGCs were prepared using electrospinning and weaving techniques. The electrospun silk fibroin fibers constituted the outer and inner layers, and the PLGA fibers formed the middle layer (**Figure 2**). The physical characteristics of the prepared ESP-NGCs are shown in **Table 1**. The voltage, SF concentration, and distance between the tip and collection rod were the main factors that affect the morphology of the

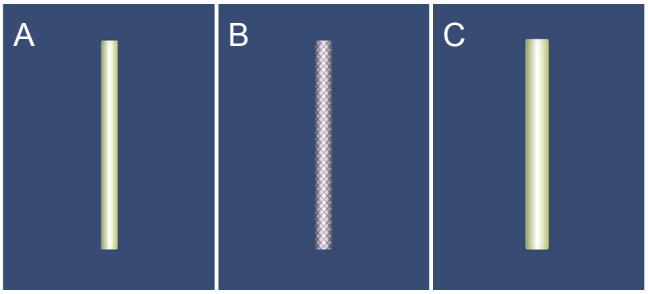

Figure 1 Schematic showing the process of making the electrospun silk fibroin (SF)/poly(lactic-co-glycolic acid) (PLGA) nerve guidance conduits (ESP-NGCs).
(A) The first layer of the conduit, the electrospun SF membrane. (B) The second layer, the PLGA net around the SF fibers. (C) The third layer, another membrane made from electrospun SF.

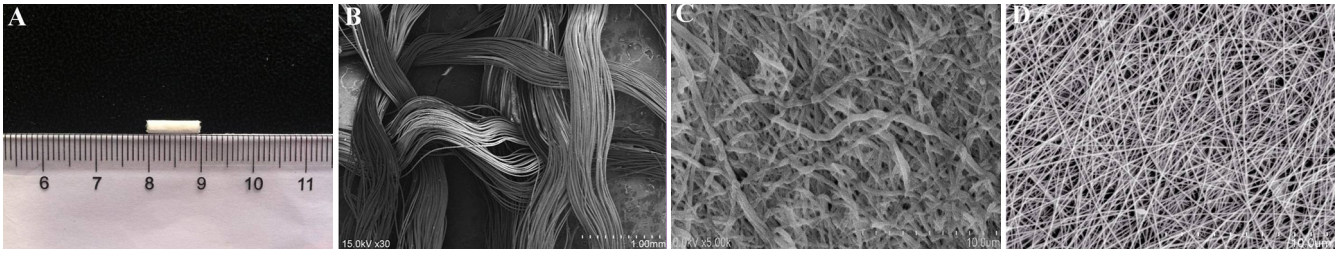

Figure 2 Micrographs of the electrospun and woven nerve guidance conduits made of silk fibroin (SF) and poly(lactic-co-glycolic acid) (PLGA) (ESP-NGC) observed under scanning electron microscopy.
(A) An external view of the conduit. (B–D) Scanning electron micrographs of the PLGA layer (B), the inner wall of the ESP-NGC (C), and electrospun SF fibers (D). Scale bars: 1.0 mm in B, 10.0 μm in C and D.

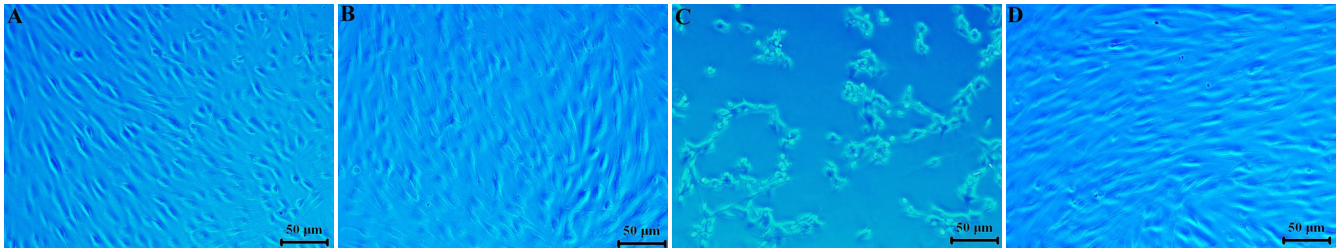

Figure 4 Brightfield images of the Schwann cells grown in hydroxyapatite (A), ESP-NGC (B), and organotin (C) extract fluids or complete medium (D) for 24 hours (inverted light microscope).
After 24 hours of culture, the Schwann cells in the hydroxyapatite (A), ESP-NGC (B), and complete medium (D) extract fluids had a long-fusiform appearance with clear edges and shining, transparent bodies. However, in the organotin extract fluid, a portion of the Schwann cells detached from the culture plate, forming large clusters and dead cells in suspension, indicating that most of those cells were dead (C).

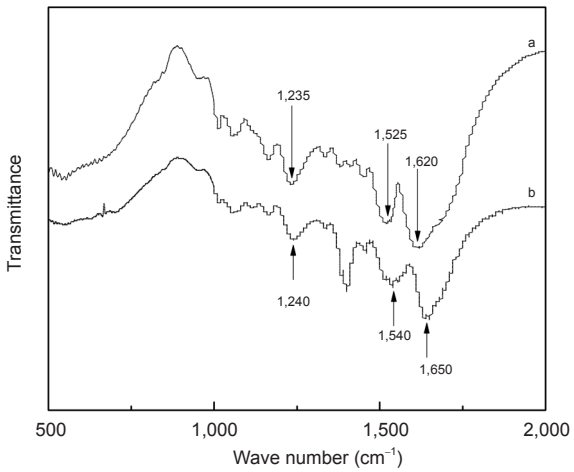

Figure 3 Fourier transform infrared (FTIR) spectra of the silk fibroin (SF).
(a) Electrospun SF treated with ethanol. (b) Electrospun SF not treated with ethanol.

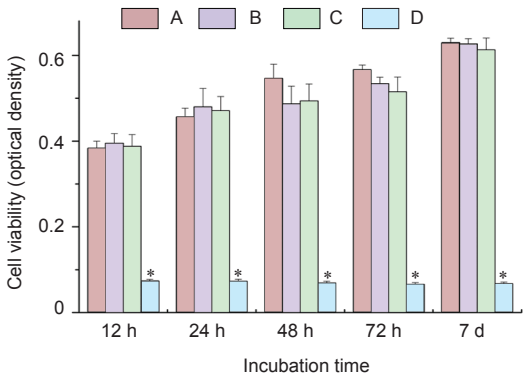

Figure 5 Viability of Schwann cells, measured by MTT assay, after culture in Dulbecco's modified Eagle medium (DMEM) complete medium (A), electrospun silk firoin/PLGA conduits (ESP-NGCs) extract fluid (B), hydroxyapatite extract fluid (C), and organotin extract fluid (D) for 12, 24, 48, and 72 hours (h) and 7 days (d).
The viability of Schwann cells cultured in the organotin extract fluid was significantly lower than that in the other culture media at all time points, while no significant difference was found among the DMEM complete medium, ESP-NGC extract, and hydroxyapatite extract fluids. In addition, the number of Schwann cells increased over time. *$P < 0.05$ *vs.* the other three culture media (one-way analysis of variance).

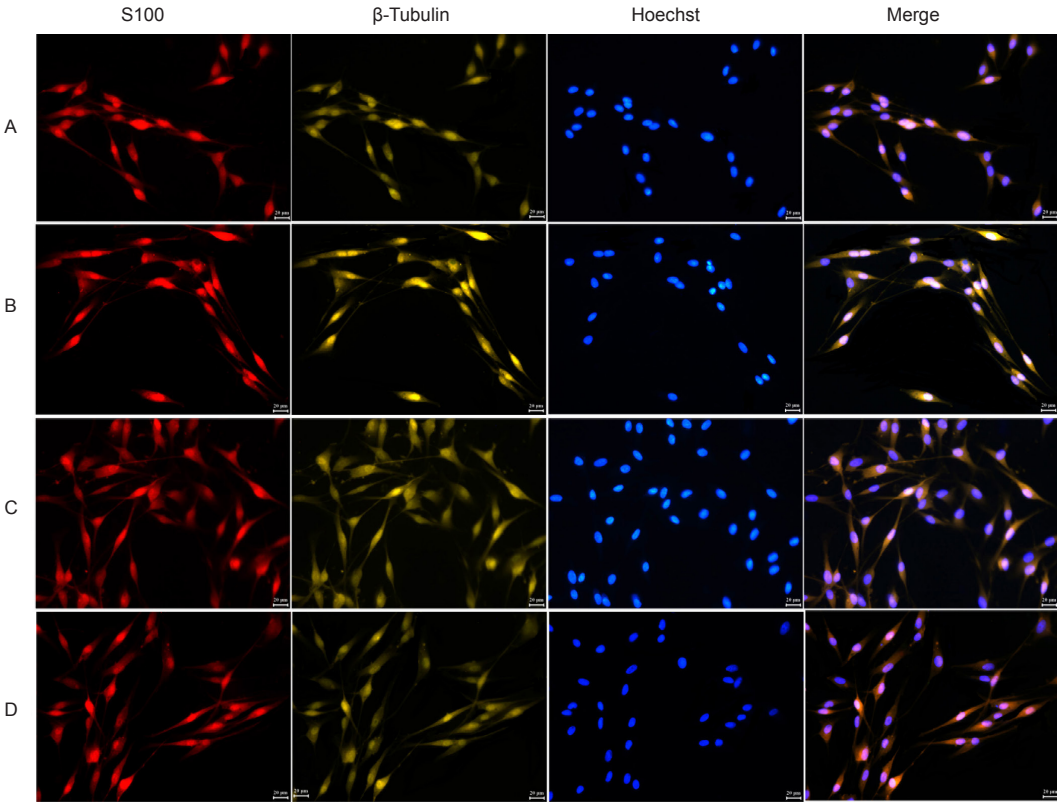

Figure 6 Immunocytochemistry of Schwann cells cultured in complete medium (A, C) and ESP-NGC extract fluid (B, D) for 1 day (A, B) and 3 days (C, D) observed with fluorescence microscopy.
S-100 staining (red), β-tubulin staining (yellow), Hoechst 33342 labeling of cell nuclei (blue), and the merged image of all three stains (last column). The expression of S-100 and the cytoskeleton of Schwann cells treated with ESP-NGC extract fluid were similar to those in cells treated with complete medium. As time passed, the cell protrusions became long and thin. Scale bars: 25 μm. ESP-NGCs: Electrospun silk fibroin/poly(lactic-co-glycolic acid) nerve guidance conduits.

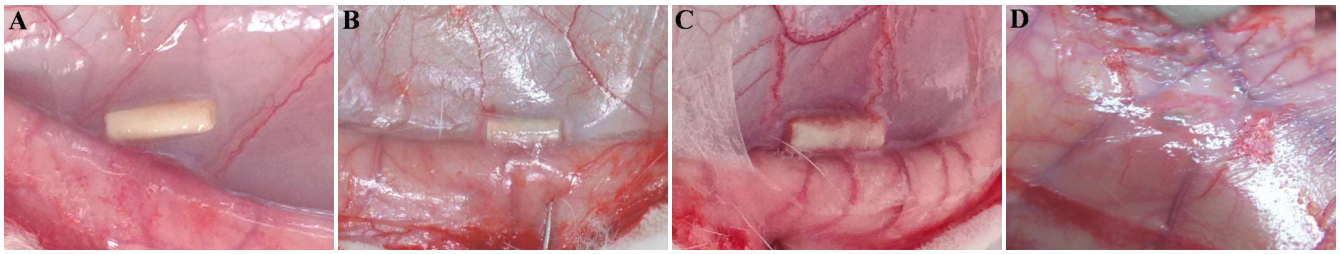

Figure 7 Photographs of the subcutaneously implanted ESP-NGCs at 4 (A), 8 (B), 12 (C), and 24 weeks (D) after surgery.
No tissue necrosis or suppuration was observed in the tissue surrounding the ESP-NGC implants, indicating a minimal tissue response to the prepared NGCs. At 4 and 8 weeks, the conduits maintained their structure intact. After 12 weeks, the conduits became smaller in size and were slightly collapsed, suggesting degradation of the conduits.

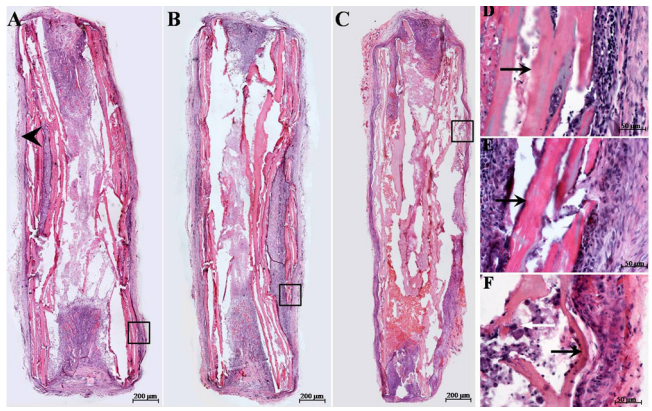

Figure 8 Light micrographs of the hematoxylin-eosin-stained ESP-NGCs at 4 (A, D), 8 (B, E), and 12 weeks (C, F) after subcutaneous implantation in rabbits.
D, E, and F show higher magnification views of the boxed areas in A, B, and C, respectively. Arrowhead: Connective tissue; black arrow and red staining: non-degraded conduits; white arrow: macrophages. Scale bars: 200 μm (A–C) and 50 μm (D–F). Thin connective tissue surrounding the conduit can be seen in A and B, with a few neutrophils and macrophages present in the lumen of the conduit. Compared to D and E, the number of macrophages in F was increased and the number of neutrophils was decreased.

Table 1 Characterization of the ESP-NGCs

Fiber radius (nm)	Inner diameter of NGC (mm)	Wall thickness (μm)	Pore size (μm)	Porosity (%)	Swelling ratio (%)
523±48	2	450±43	6–8	79.95±1.02	65.23±0.93

ESP-NGCs: Electrospun silk fibroin (SF)/poly(lactic-co-glycolic acid) (PLGA) nerve guidance conduits; NGCs: nerve guidance conduits.

fibers. In the last experiment of the present study, a voltage of 23 kV, solution concentration of 15%, and 12 cm distance were used.

Conformational changes in the SF

In order to identify conformational changes in the SF, FTIR spectroscopy was performed. The IR spectra of the electrospun SF are shown in **Figure 3**. The amide I, amide II, and amide III bands of the electrospun SF were clearly observed at 1,650, 1,540, and 1,240 cm^{-1}, which are the characteristic peaks of the random coil conformation of electrospun SF before ethanol treatment. The electrospun SF treated with ethanol showed strong adsorption bands at 1,620 (amide I), 1,525 (amide II), and 1,235 cm^{-1} (amide III), which are attributed to the β-sheet conformation (Zhang et al., 2013). Ordered crystallites formed after ethanol treatment. Although many researchers have used methanol to induce conformational changes in SF (Santin et al., 1999; Min et al., 2004; Zhou et al., 2010), methanol is toxic and it is harmful to the nervous system, respiratory system, and eyes. Thus, ethanol is increasingly used instead of methanol (Bhattacharjee et al., 2013; Fan et al., 2014; Qian et al., 2014).

Mechanical properties of the ESP-NGCs

The resistance of the NGC to sutures being pulled out is a meaningful piece of information for clinical application. In addition, NGCs should have sufficient mechanical strength to protect the regenerating axons from invasion by the surrounding connective tissue (Wang et al., 2008). The results of the mechanical testing indicated that the mechanical properties of the ESP-NGCs were sufficient. The maximum fracture strength of the ESP-NGC was 5.4 ± 0.5 MPa, recorded at the point when the outer layer fractured. The compressive strength was 9.51 ± 1.06 N.

Biocompatibility *in vitro*

Rat Schwann cells cultured in ESP-NGC extracts

Light microscopy was used to visualize the growth of the rSCs in the four different culture mediums: hydroxyapatite extract fluid, ESP-NGC extract fluid, organotin extract fluid, and complete medium. After 24 hours in culture, no significant differences were found in terms of the cell morphology among the hydroxyapatite extract fluid, ESP-NGC extract fluid, and the complete medium. The Schwann cells had a long fusiform shape with clear edges and shining, transparent bodies. However, a portion of the Schwann cells in the organotin extract fluid detached from the culture plate, and there were large clusters and dead cells suspended, indicating that most of the cells died (**Figure 4**). These results suggest that the ESP-NGC extract, unlike the organotin extract, has no cytotoxicity to the cultured Schwann cells.

Viability of the Schwann cells

The MTT assay is widely performed to assess cytotoxicity by determining cell viability, and the results of the MTT assay are shown in **Figure 5**. The viability of the Schwann cells cultured in the ESP-NGC extract was not significantly different than that of cells cultured in hydroxyapatite extract fluid or complete medium after 12, 24, 48, and 72 hours or 7 days. On the contrary, the viability of the Schwann cells cultured in the organotin extract fluid was significantly lower than that in each of the other culture mediums at all time points. In addition, the number of Schwann cells increased over time. The MTT results indicated that the ESP-NGC extract had no effect on the survival or proliferation of the Schwann cells cultured in it.

ESP-NGC extract was not cytotoxicity to the cultured Schwann cells

The protein S-100 mainly exists in Schwann cells of the peripheral nervous system and in glia in the central nervous system. Mata et al. (1990) found that the amount of S-100 protein in Schwann cells was correlated with the thickness of the myelin sheath. As a type of cytoskeletal protein, β-tubulin is often used to observe the microtubules of cells. The expression of S-100 and the cytoskeleton of the Schwann cells treated with ESP-NGC extract fluid was similar to those of cells treated with complete medium, as shown in **Figure 6**. Further, the ESP-NGC extract fluid facilitated the adhesion and growth of the Schwann cells. We can see in **Figure 6** that as time passed, the cell protrusions became long and thin. The immunocytochemistry also suggests that the ESP-NGC extract was not cytotoxic to the cultured Schwann cells.

Biocompatibility *in vivo*

Gross appearance of the conduit after implantation

The subcutaneous implants were harvested at 4, 8, 12, and 24 weeks. By gross observation, the ESP-NGCs were still present in every animal examined at 12 weeks. No peri-implant tissue necrosis or suppuration was observed around the ESP-NGCs in the recipient tissue at any time point, indicating that the tissue response to the prepared NGCs was minimal. In addition, as shown in **Figure 7**, as time passed, the conduits gradually became smaller in size and finally collapsed. Most of the conduits had been degraded by 24 weeks.

Morphological changes in the ESP-NGCs

Artificial implants can promote and guide axonal growth, as well as the migration of Schwann cells, and they often induce

excessive inflammatory reactions (Allmeling et al., 2008). At each time point, the harvested ESP-NGCs were sectioned, stained with hematoxylin-eosin, and examined under light microscopy, which showed a number of morphological changes in the ESP-NGCs over tie (**Figure 8**). At 4 weeks, a thin connective tissue had formed that was mainly composed of hyperplastic fibroblasts packing near and surrounding the conduit wall. Neutrophil infiltration and macrophages were seen in the lumen of the conduit. A small amount of ingrown fibrous connective tissue began to appear in the conduit ends. At 8 weeks, the connective tissue was slightly thicker, and the hyperplastic fibroblasts, neutrophils, and macrophages appeared similar to those at 4 weeks. At 12 weeks, the connective tissue around the conduit wall had become thinner again. The number of infiltrated neutrophils was decreased, while the number of macrophages was increased and a few lymphocytes were found. More ingrowth of fibrous connective tissue in the conduit ends was present, indicating mild rejection or an inflammatory reaction. Neovascularization not only increases the degradation and absorption of the NGCs, but also provides nutrition for the process of nerve regeneration. At 24 weeks, no intact ESP-NGCs were recovered because they had all fragmented. Together, these results show that a slight inflammatory reaction appeared during the early stage, but it was short lived, suggesting that the ESP-NGCs are biocompatible *in vivo*.

Discussion

Peripheral nerve regeneration and functional recovery are strongly dependent on the scaffold properties. SF has been used in medical fields for a long time because it is biocompatible and has appropriate mechanical properties. Electrospinning is an easy and efficient technique for fabricating scaffolds with nanoscale dimensions and high porosity. Layers of electrospun SF nanofibers are architecturally similar to native collagen structures formed by extracellular matrix proteins. Collagen fibers and their nanoscale architecture are composed of multiple fibrils arranged in a three-dimensional network structure together with proteoglycans (Min et al., 2004). Here, we used electrospun SF as the outer and inner layers, which can promote the attachment and spreading of cells and guide nerve regeneration. The high porosity and interconnected porous structure of the ESP-NGCs offers a large capacity for material exchange *in vivo*, which is necessary to meet the nutritional requirements for peripheral nerve regeneration. In addition, materials with a high specific surface area and highly porous three-dimensional structure are desirable for high-density cell and tissue cultures because they provide a biological environment that is conducive to cell adhesion, growth, proliferation, and the transport of nutrients and metabolic waste.

For NGCs, the mechanical properties are often as important as the biocompatibility. We used a PLGA net in the middle layer to increase the mechanical strength and maintain sufficient luminal space for axons to grow across. Tests in animals have demonstrated that ESP-NGCs, as prepared here, can withstand a suture thread being pulled out of them. Furthermore, these strong mechanical properties allow the ESP-NGC to resist muscular contraction and maintain its cylindrical shape for considerable periods of time after implantation, thus providing sufficient three-dimensional space for nerve regeneration.

Schwann cells are the principle glial cells of the peripheral nervous system, and they make significant contributions to the regenerative process. Schwann cells are able to wrap around the axons of motor and sensory neurons to form compact myelin sheaths, guide axon growth, and secrete various growth factors to create a microenvironment favorable to nerve regeneration (Krekoski et al., 2001; Yang et al., 2007a; Gu et al., 2012). Therefore, it is important to perform cytotoxicity testing as suggested by the International Standards compiled in ISO 10993-5. We cultured Schwann cells in different extracts, including the ESP-NGC extract and a control extract. The morphology, viability, and immunochemistry data all showed that the ESP-NGC extract could support the adhesion, growth, and proliferation of Schwann cells, suggesting that the ESP-NGC was not cytotoxic to the cultured Schwann cells.

After implantation *in vivo*, few neutrophils, lymphocytes, and macrophages were found at 1 month after implantation, suggesting that the ESP-NGCs induced a slight inflammatory reaction, but showed no obvious rejection. As time passed, more fibrous tissues were generated in the lumen of the ESP-NGCs and the size of implants gradually decreased, indicating that the ESP-NGCs were biocompatible and had favorable degradation characteristics.

Conclusion

In this study, we developed a type of NGC using electrospinning and weaving. The net structure in the middle layer imbued the NGC with favorable mechanical strength, making it strong enough to resist the suture being pulled out of it. Both *in vivo* and *in vitro* experiments showed that the designed NGC was biocompatible. All the results indicate that this novel NGC may be useful as an alternative to nerve autografts.

Author contributions: *YLW designed the study, performed experiments, and wrote the paper. QLF and YK performed experiments. YMY designed the study and revised the paper. XMG collected and analyzed the data. All authors approved the final version of the paper.*

Conflicts of interest: *None declared.*

References

Allmeling C, Jokuszies A, Reimers K, Kall S, Choi CY, Brandes G, Kasper C, Scheper T, Guggenheim M, Vogt PM (2008) Spider silk fibres in artificial nerve constructs promote peripheral nerve regeneration. Cell Proliferat 41:408-420.

Altman GH, Diaz F, Jakuba C, Calabro T, Horan RL, Chen JS, Lu H, Richmond J, Kaplan DL (2003) Silk-based biomaterials. Biomaterials 24:401-416.

Bayraktar O, Malay O, Ozgarip Y, Batigun A (2005) Silk fibroin as a novel coating material for controlled release of theophylline. Eur J Pharm Biopharm 60:373-381.

Bhattacharjee M, Schultz-Thater E, Trella E, Miot S, Das S, Loparic M, Ray AR, Martin I, Spagnoli GC, Ghosh S (2013) The role of 3D structure and protein conformation on the innate and adaptive immune responses to silk-based biomaterials. Biomaterials 34:8161-8171.

Chen C, Cao C, Ma X, Tang Y, Zhu H (2006) Preparation of non-woven mats from all-aqueous silk fibroin solution with electrospinning method. Polymer 47:6322-6327.

Chen X, Yang Y, Wu J, Zhao Y, Ding F, Gu X (2007) Biocompatibility studies of silk fibroin-based artificial nerve grafts in vitro and in vivo. Prog Nat Sci 17:1029-1034.

Choi JS, Lee SJ, Christ GJ, Atala A, Yoo JJ (2008) The influence of electrospun aligned poly(epsilon-caprolactone)/collagen nanofiber meshes on the formation of self-aligned skeletal muscle myotubes. Biomaterials 29:2899-2906.

Dal Pra I, Freddi G, Minic J, Chiarini A, Armato U (2005) De novo engineering of reticular connective tissue in vivo by silk fibroin nonwoven materials. Biomaterials 26:1987-1999.

Ducker TB, Hayes GJ (1970) Peripheral nerve grafts: experimental studies in the dog and chimpanzee to define homograft limitations. J Neurosurg 32:236-243.

Evans GR (2000) Challenges to nerve regeneration. Semin Surg Oncol 19:312-318.

Fabre T, Schappacher M, Bareille R, Dupuy B, Soum A, Bertrand-Barat J, Baquey C (2001) Study of a (trimethylenecarbonate-co-epsilon-caprolactone) polymer--part 2: in vitro cytocompatibility analysis and in vivo ED1 cell response of a new nerve guide. Biomaterials 22:2951-2958.

Fan L, Cai Z, Zhang K, Han F, Li J, He C, Mo X, Wang X, Wang H (2014) Green electrospun pantothenic acid/silk fibroin composite nanofibers: fabrication, characterization and biological activity. Colloids Surf B Biointerfaces 117:14-20.

Félix Lanao RP, Leeuwenburgh SC, Wolke JG, Jansen JA (2011) In vitro degradation rate of apatitic calcium phosphate cement with incorporated PLGA microspheres. Acta Biomater 7:3459-3468.

Fini M, Motta A, Torricelli P, Glavaresi G, Aldini NN, Tschon M, Giardino R, Migliaresi C (2005) The healing of confined critical size cancellous defects in the presence of silk fibroin hydrogel. Biomaterials 26:3527-3536.

Gotoh Y, Niimi S, Hayakawa T, Miyashita T (2004) Preparation of lactose-silk fibroin conjugates and their application as a scaffold for hepatocyte attachment. Biomaterials 25:1131-1140.

Gu Y, Ji Y, Zhao Y, Liu Y, Ding F, Gu X, Yang Y (2012) The influence of substrate stiffness on the behavior and functions of Schwann cells in culture. Biomaterials 33:6672-6681.

Guo J, Gao X, Su L, Xia H, Gu G, Pang Z, Jiang X, Yao L, Chen J, Chen H (2011) Aptamer-functionalized PEG-PLGA nanoparticles for enhanced anti-glioma drug delivery. Biomaterials 32:8010-8020.

Jin HH, Min SH, Song YK, Park HC, Yoon SY (2010) Degradation behavior of poly(lactide-co-glycolide)/beta-TCP composites prepared using microwave energy. Polym Degrad Stab 95:1856-1861.

Kim MS, Ahn HH, Shin YN, Cho MH, Khang G, Lee HB (2007) An in vivo study of the host tissue response to subcutaneous implantation of PLGA- and/or porcine small intestinal submucosa-based scaffolds. Biomaterials 28:5137-5143.

Kim UJ, Park J, Kim HJ, Wada M, Kaplan DL (2005) Three-dimensional aqueous-derived biomaterial scaffolds from silk fibroin. Biomaterials 26:2775-2785.

Krekoski CA, Neubauer D, Zuo J, Muir D (2001) Axonal regeneration into acellular nerve grafts is enhanced by degradation of chondroitin sulfate proteoglycan. J Neurosci 21:6206-6213.

Lee JY, Bashur CA, Goldstein AS, Schmidt CE (2009) Polypyrrole-coated electrospun PLGA nanofibers for neural tissue applications. Biomaterials 30:4325-4335.

Mata M, Alessi D, Fink DJ (1990) S100 is preferentially distributed in myelin-forming Schwann cells. J Neurocytol 19:432-442.

Min BM, Lee G, Kim SH, Nam YS, Lee TS, Park WH (2004) Electrospinning of silk fibroin nanofibers and its effect on the adhesion and spreading of normal human keratinocytes and fibroblasts in vitro. Biomaterials 25:1289-1297.

Qian JM, Suo AL, Jin XX, Xu WJ, Xu MH (2014) Preparation and in vitro characterization of biomorphic silk fibroin scaffolds for bone tissue engineering. J Biomed Mater Res A 102:2961-2971.

Santin M, Motta A, Freddi G, Cannas M (1999) In vitro evaluation of the inflammatory potential of the silk fibroin. J Biomed Mater Res 46:382-389.

Shao Z, Vollrath F (2002) Surprising strength of silkworm silk. Nature 418:741-741.

Suzuki K, Suzuki Y, Tanihara M, Ohnishi K, Hashimoto T, Endo K, Nishimura Y (2000) Reconstruction of rat peripheral nerve gap without sutures using freeze-dried alginate gel. J Biomed Mater Res 49:528-533.

Tang X, Ding F, Yang Y, Hu N, Wu H, Gu X (2009) Evaluation on in vitro biocompatibility of silk fibroin-based biomaterials with primarily cultured hippocampal neurons. J Biomed Mater Res A Part A 91:166-174.

Uebersax L, Fedele DE, Schumacher C, Kaplan DL, Merkle HP, Boison D, Meinel L (2006) The support of adenosine release from adenosine kinase deficient ES cells by silk substrates. Biomaterials 27:4599-4607.

Unger RE, Peters K, Wolf M, Motta A, Migliaresi C, Kirkpatrick CJ (2004) Endothelialization of a non-woven silk fibroin net for use in tissue engineering: growth and gene regulation of hunian endothelial cells. Biomaterials 25:5137-5146.

Vozzi G, Flaim C, Ahluwalia A, Bhatia S (2003) Fabrication of PLGA scaffolds using soft lithography and microsyringe deposition. Biomaterials 24:2533-2540.

Wang W, Itoh S, Matsuda A, Ichinose S, Shinomiya K, Hata Y, Tanaka J (2008) Influences of mechanical properties and permeability on chitosan nano/microfiber mesh tubes as a scaffold for nerve regeneration. J Biomed Mater Res A 84:557-566.

Wang XD, Hu W, Cao Y, Yao J, Wu J, Gu XS (2005) Dog sciatic nerve regeneration across a 30-mm defect bridged by a chitosan/PGA artificial nerve graft. Brain 128:1897-1910.

Weber RA, Breidenbach WC, Brown RE, Jabaley ME, Mass DP (2000) A randomized prospective study of polyglycolic acid conduits for digital nerve reconstruction in humans. Plast Reconstr Surg 106:1036-1045; discussion 1046-1048.

Weinstein DE, Wu R (2001) Isolation and purification of primary Schwann cells. Curr Protoc Neurosci Chapter 3:Unit 3.17.

Yamada H, Igarashi Y, Takasu Y, Saito H, Tsubouchi K (2004) Identification of fibroin-derived peptides enhancing the proliferation of cultured human skin fibroblasts. Biomaterials 25:467-472.

Yang Y, Chen X, Ding F, Zhang P, Liu J, Go X (2007a) Biocompatibility evaluation of silk fibroin with peripheral nerve tissues and cells in vitro. Biomaterials 28:1643-1652.

Yang Y, Ding F, Wu H, Hu W, Liu W, Liu H, Gu X (2007b) Development and evaluation of silk fibroin-based nerve grafts used for peripheral nerve regeneration. Biomaterials 28:5526-5535.

Yang Y, Zhao Y, Gu Y, Yan X, Liu J, Ding F, Gu X (2009) Degradation behaviors of nerve guidance conduits made up of silk fibroin in vitro and in vivo. Polym Degrad Stab 94:2213-2220.

Yuan Y, Zhang PY, Yang YM, Wang X, Gu XS (2004) The interaction of Schwann cells with chitosan membranes and fibers in vitro. Biomaterials 25:4273-4278.

Zhang Q, Li M, Xu W, Li J, Yan S (2013) A novel silk fibroin scaffolds with oriented multichannels. Mater Lett 105:8-11.

Zhou JA, Cao CB, Ma XL, Hu L, Chen LA, Wang CR (2010) In vitro and in vivo degradation behavior of aqueous-derived electrospun silk fibroin scaffolds. Polym Degrad Stab 95:1679-1685.

Copyedited by McCarty W, Robens J, Li CH, Song LP, Zhao M